Journal of Engineering Physics and Thermophysics, Vol. 75, No. 1, 2002

FEATURES OF SEGREGATION OF DOPING IMPURITIES OF V(a) SUBGROUP ELEMENTS ON ANGULAR CONFIGURATIONS OF THE SILICON/SILICON DIOXIDE OXIDATION BOUNDARY

G. A. Tarnavskii,[a] S. I. Shpak,[a] and M. S. Obrecht[b]

UDC 519.6:541.1

On the basis of computer simulation of the physicochemical process of segregation of doping impurities implanted in the basic material (silicon), the features of ejection of V(a) subgroup elements (phosphorus, arsenic, and antimony) on the angular configurations of the silicon/silicon dioxide oxidation boundary are investigated.

Computer simulation of segregation — the physicochemical process of interaction of the basic material oxidation wave (boundary) with doping impurities of various chemical materials implanted in this basic material (base) — is an important component of the simulation of a complex problem connected with the development of materials having required semiconductor properties. The physical mechanism of segregation is determined by the appearance at the oxide/material boundary of an electromagnetic field with a narrowly localized short-duration high-intensity potential ejecting (ejection-type segregation) or injecting (injection-type segregation) depending on the configuration of the outer electron shells of the doping chemical elements.

In the present paper, the segregation of V(a) subgroup elements, phosphorous P-15 ($3s^2 3p^3$), arsenic As-33 ($4s^2 4p^3$), and antimony Sb-51 ($5s^2 5p^3$), implanted in silicon Si-14 ($3s^2 3p^2$) is investigated. Enclosed in brackets are the configurations of the electronic shells of elements whose structure determines the process of strong ejection (pushing out) of P, As, and Sb at the Si/SiO_2 wave from the SiO_2 oxide into the Si material. The quantum-mechanical approach to the solution of this problem is faced with great difficulties and practically cannot be realized even with the use of modern computer facilities. This calls for approximate models of segregation. The proposed computation cycle uses the theoretical model and the computer algorithm realizing it described in detail in [1], which also shows the place of this model among the other segregation models in use [2–7]. The segregation of doping impurities at the Si/SiO_2 boundary caused by the process of thermochemical oxidation of silicon is characterized (see, for example, [8]) by the segregation coefficient m, whose thermodynamic estimation yields values to an accuracy of one to two orders of magnitude, while the direct experimental measurements made by different authors show considerable differences in the value depending on the oxidation conditions. In the computations presented below, for P, As, and Sb, the value of $m = 200$ corresponding to the universally accepted value for thermodynamically equilibrium segregation was assumed. (Note that nonequilibrium can decrease the value of m to 30.)

Generally speaking, numerical simulation of semiconductor properties of silicon with doping impurities is mainly carried out with a complex consideration of several processes: implantation of impurities in the basic material, its oxidation, segregation of impurities at the oxidation wave boundary, and diffusion of an

[a]Institute of Theoretical and Applied Mechanics, Siberian Branch of the Russian Academy of Sciences, Novosibirsk; email: shpak@itam.nsc.ru; [b]University of Waterloo, Ontario, Canada; email: obrecht@siborg.ca. Translated from Inzhenerno-Fizicheskii Zhurnal, Vol. 75, No. 1, pp. 142–147, January–February, 2002. Original article submitted April 3, 2001.

 1062-0125/02/7501-0190$27.00

impurity in the oxide and material. In the simplest cases, the results of calculations of such a complex problem correlate with experimental data with a more or less acceptable accuracy. In complex problems (in particular, with considerably curvilinear boundaries of oxidation), interpretation of the results obtained can be very difficult, because it becomes unclear which of the above processes is simulated with a sufficient accuracy and which is not. For example, an insufficiently good calculation of the segregation process having an oscillatory character can be veiled by the diffusion calculation having high smoothing properties. In our opinion, this makes it absolutely necessary to separately develop the numerical simulation of different physical processes for the possibility of adequate comparison with experimental results of the type of [9, 10] on the path toward elaborating new technologies for obtaining semiconductor materials.

Formulation of the Problem. We consider the process of segregation of V(a) subgroup elements implanted in silicon with oxide waves moving in it. The Si/SiO_2 boundaries have rectangular kinks of the generating line forming four types of configurations of the oxide in the material: "forward and backward steps" and cavities of the "trench" and "square" types (see Figs. 1a, 2a, 3a, and 4a). The initial distribution of impurities in Si is assumed to be homogeneous, and the diffusion of impurities is not taken into account.

The dimensional parameters of the problem are as follows: the length and width of the Si base (calculated area x–y) is from 0.5 to 1.5 μm; the minimum initial and the maximum finite thicknesses of the oxide are 0.001 and 0.8, respectively; the oxidation rate is 0.005 μm/min at a pressure of free O_2 of 10^5 Pa and an oxidation temperature of 1100^oC; the initial impurity concentrations are from 10^{16} to 10^{22} cm^{-3}. In the calculations, we normalized the linear sizes to 1 μm, the time to 1 min, and the concentrations to 10^{20} cm^{-3} to provide, if necessary, dimensionless-to-dimensional conversion of obtained information.

Segregation on the Forward Step. Numerical simulation of segregation is carried out, as a rule, for an oxidation wave boundary having a smooth character (continuous first and second coordinate derivatives) of the type of a "bird's beak" (see, for example, [7]). In making calculations, this also provides smooth distributions of impurity concentrations in front of and behind the segregation front in its tangent direction. In practice, however, in developing technologies for constructing semiconductor materials with given properties in the base it is necessary to use grooves of various rectangular configurations, which leads, respectively, to configurations of oxide/material boundaries also having right angles (in the real sense — parts with a very large change in the curvature, in the formal sense — having breaks of the first derivatives). Calculation of the segregation is, on the one hand, a good test for computation methods and computer programs realizing them and, on the other hand, the obtained numerical results are very interesting from the physical point of view and are of great practical importance.

Figure 1 shows some of the results of the numerical simulation of the dynamics of the process of segregation of impurities at the Si/SiO_2 oxidation wave having the form of a forward step. Figure 1a presents the topology of the problem: the shaded portion is occupied by SiO_2, whose boundary moves uniformly from the origin of coordinates into the bulk of the Si material, ejecting in front of it an impurity of the type of P, As, or Sb implanted in Si. Figure 1b illustrates the impurity distribution $C(x, y)$ in the base (the far angle in Fig. 1b corresponds to the origin of coordinates in Fig. 1a): at the oxide boundary, a narrowly localized wall-like front of the impurity concentration arises. One can clearly see the "ship stem" effect — a characteristic configuration of the "displaced water splash" with the minimum value at the boundary kink and its sharp increase to the left and to the right of the kink along the flat portion of the boundary. Note that this impurity configuration is the initial condition for the functioning of the diffusion calculation algorithm on a given time layer, and we can forecast high diffusion flows not only transverse to the segregation front but also along it. However, this places special requirements upon the quality of diffusion calculation in a given subarea and the methods of performing it with the necessity of densening the calculation net in two coordinate directions in the areas of large $C(x, y)$ gradients, which, taking into account the motion dynamics of the boundary, may turn out to be an unduly excessive and difficult-to-realize demand in organizing the solution of the whole problem with the calculation of the processes of implantation, oxidation, segregation, and diffusion.

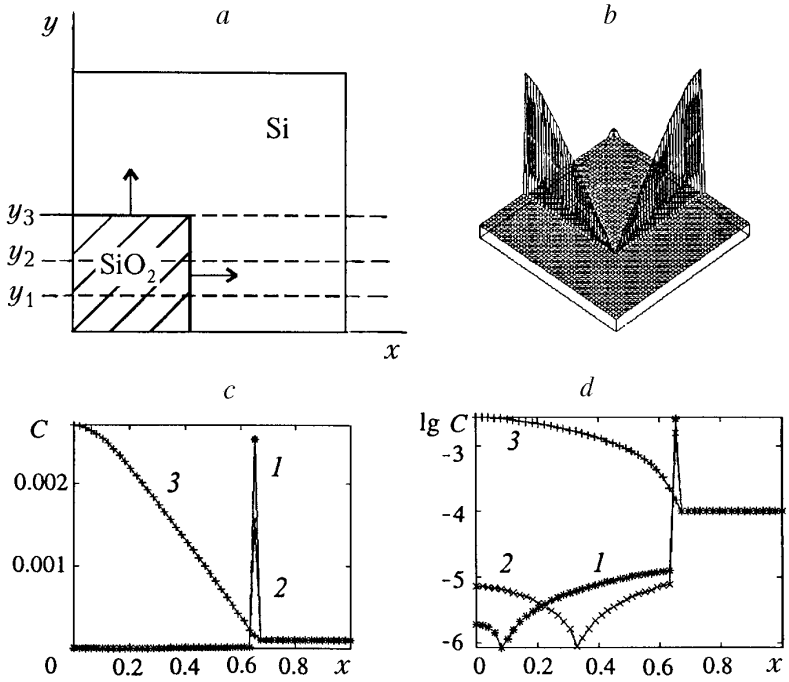

Fig. 1. Segregation on the forward step: a) general topology of the problem; b) isometry of $C(x, y)$ concentrations in the calculated area; c) $C(x, y_i)$ distributions, i = 1, 2, 3; d) log ($C(x, y_i)$) distributions. 1–3 correspond to the values of $y_1 = 0.12$, $y_2 = 0.25$, and $y_3 = 0.5$.

Figure 1c permits exact quantitative analysis of the solution of the segregation problem. It shows one-dimensional distributions of impurity concentrations $C(x)$ at certain fixed values of y_1, y_2, and y_3 given by the dashed lines in Fig. 1a. The concentration distributions on curves 1 and 2 have three characteristic sections: the concentration in the SiO_2 oxide ($x < 0.62$), the concentration peak at the segregation wave ($x_* = 0.64$), and the initial concentration in the Si material ($x > 0.66$). The intensities of the $C(x_*, y_1)$ and $C(x_*, y_2)$ peaks reach values of $2.51 \cdot 10^{-3}$ and $1.52 \cdot 10^{-3}$. Curve 3 presents the distributions of $C(x, y_3)$ concentrations directly on the straight portion of the oxidation wave moving towards an increase in y and is in the range of $x < 0.63$, figuratively speaking, a "set of peaks" analogous to the peaks of curves 1 and 2. Here a rather sharp decrease in the $C(x)$ values towards the corner (kink) of the oxidation boundary, from $2.74 \cdot 10^{-3}$ to the unperturbed value of 10^{-4}, is characteristic. The seemingly uniform $C(x, y_1)$ and $C(x, y_2)$ distribution in the oxide ($x < 0.62$) is actually not uniform. For more detailed analysis Fig. 1d presents the same data but on a logarithmic scale. We can note a small increase in $C(x)$ from the oxide depth to its boundary, i.e., the segregation wave "ejects" from the oxide into the material the quantity of impurity determined by a law which, though immaterial, decreases with moving SiO_2/Si boundary. The kinks of curves 1 and 2 in the region of the oxide show its initial configuration at time $t = 0$.

Segregation on the Backward Step. This process (see Fig. 2a) seems to be the reverse of the process of segregation on the forward step in the sense that although the SiO_2/Si oxidation wave ejects doping impurities of the type of P, As, and Sb from the SiO_2 oxide into the Si material, the configuration of the ejected mass is completely different: the "ship stem" effect is replaced by the "bulldozer" effect when, as the SiO_2/Si boundary moves, in its corner (see Fig. 2a) more and more impurity mass collects. Figure 2b clearly illustrates this effect: the $C(x, y)$ concentration peak in the corner by the presented instant of time is so large that the $C(x, y)$ distribution peaks in the other, adjacent sections of the SiO_2/Si front, as compared to it, seem to be small, although they are very significant compared to the background values of $C(x, y)$ in the oxide depth and the unperturbed initial values in the material.

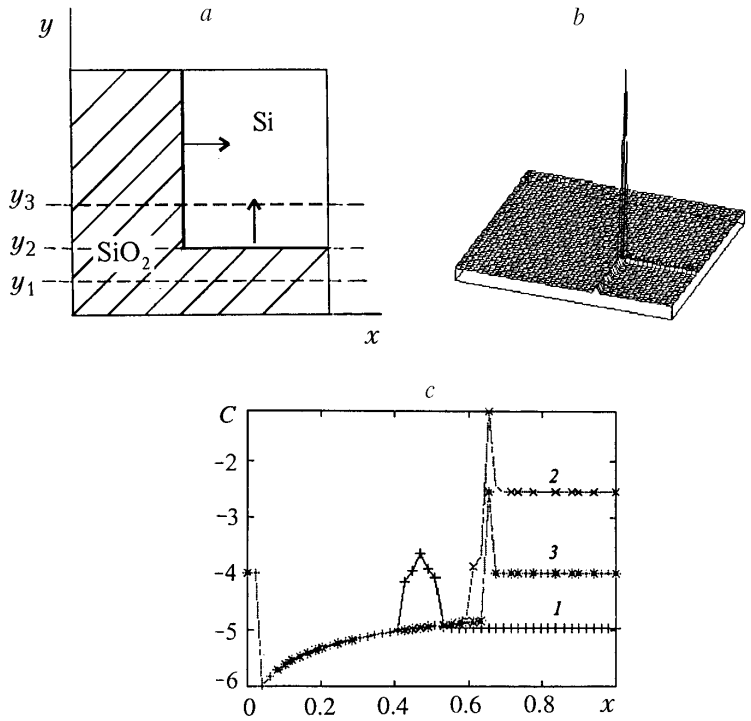

Fig. 2. Segregation on the backward step: a) general topology of the problem; b) isometry of $C(x, y)$ concentrations in the calculated area; c) log ($C(x, y_i)$) distributions. 1–3 correspond to Fig. 1.

The logarithmic scale of Fig. 2c permits quantitative analysis of the field of $C(x, y)$ concentrations in the calculated area. Curve 2, presenting the $C(x, y_2)$ distribution along the right-hand edge of the front going towards an increase in the y-coordinate, has four characteristic sections. The first section ($x < 0.025$) is the area of the initial position of the oxide; beginning from time $t = 0$, the segregation ejects the impurity from the point $x = 0.025$ to the right. The second section ($0.025 < x < 0.66$) is the oxide area that has arisen in the period from $t = 0$ to $t = 40$ (by the moment the counting is completed and the obtained results are presented). The weak increase in $C(x, y_2)$ with increasing x in this range is analogous to that described above and is due to the small decrease in the segregation ejection with moving SiO_2/Si boundary. The peak of the $C(x, y_2)$ value at $x = 0.66$ is attained in the third section — in the corner of the boundary where a considerable portion of the impurity displaced from the oxide collects. The fourth section ($x > 0.68$) is a flat front of the segregation wave ejecting upwards the impurity in the y-direction. This section is characterized by a high, but even value of $C(x, y_2)$.

Curve 3 (see Fig. 2c) illustrates the values of $C(x, y_3)$ on the ray passing above the corner point and also having four sections: two sections in SiO_2, at the SiO_2/Si front, and in Si. The $C(x, y_3)$ peak is, naturally, situated where the $C(x, y_2)$ peak is — at $x = 0.66$, but its intensity is about two orders of magnitude lower. In the first and second ($x < 0.66$) sections, the $C(x, y_3)$ distribution practically completely coincides with the $C(x, y_2)$ distribution. The fourth section ($x < 0.68$) passes through the unperturbed field and here the $C(x, y_3)$ values are equal to the initial values (10^{-4}).

Curve 1 (see Fig. 2c) passes through the oxide area and illustrates the whole prehistory of the SiO_2/Si boundary motion to the "right–upwards." The $C(x, y_1)$ values are very small; they are one to two orders of magnitude lower than the initial values. There is a concentration peak dislocated at the point of intersection of the mechanical trajectory of the SiO_2/Si boundary corner with the ray $y_1 = 0.12$ due to the fact that, moving in the calculated area, the superpeak (see Fig. 2b) leaves in the oxide its trace in the form of subareas of somewhat heightened values of concentrations practically reaching the background values of 10^{-4}.

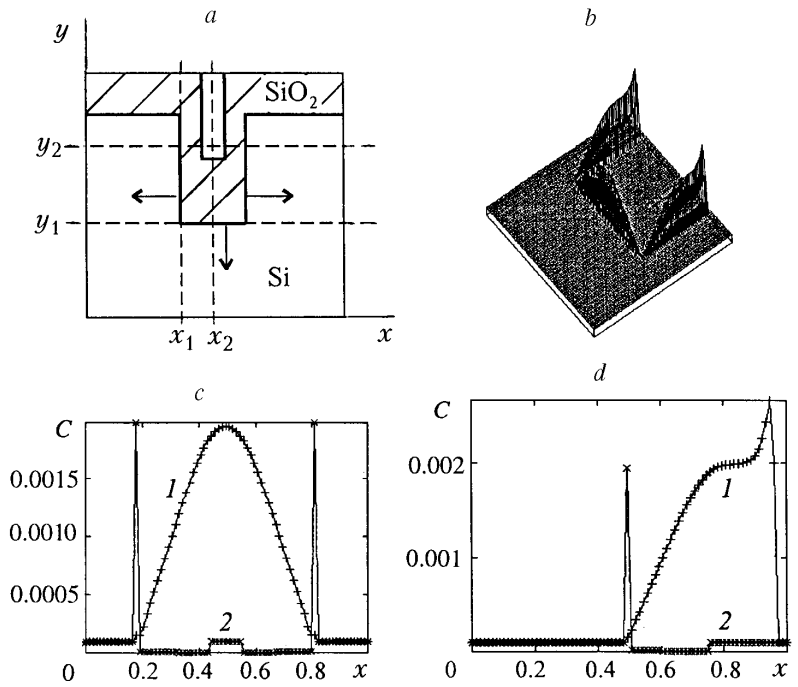

Fig. 3. Segregation on the "trench"-type cavity: a) general topology of the problem; b) isometry of $C(x, y)$ concentrations in the calculated area; c) log ($C(x, y_i)$) distributions (1 and 2 correspond to $y_1 = 0.5$ and $y_2 = 0.75$); d) $C(x_i, y)$ concentrations (1 and 2 correspond to $x_1 = 0.2$ and $x_2 = 0.5$).

Segregation on the "Trench"-Type Cavity. The process of segregation of impurities on such a type of configuration of the oxidation boundary (see Fig. 3a), which is very close to those used in the technologies for developing semiconductor materials, has characteristic features typical of the above-considered segregation processes on the forward and backward steps. Figure 3b adequately illustrates, in terms of quality, the structures of displacing impurities from the oxide into the material that are formed at the SiO_2/Si boundaries: straight $C(x, y)$ "walls" at the boundaries of oxidation wave motion, which have "troughs" toward the vertices of the convex corners (the "ship stem" effect) and peaks in the vertices of the concave corners (the "bulldozer" effect).

A quantitative analysis of the $C(x, y)$ concentration distribution in the calculated area can be carried out on one-dimensional graphs of $C(x, y)$ sections by rays y = const and x = const (Fig. 3c, d). Curve 1 in Fig. 3c, presenting the $C(x, y_1)$ values, passes along the SiO_2/Si front (see Fig. 3a), with its central section ($0.2 < x < 0.8$) lying at the front proper and its left- ($x < 0.2$) and right-hand ($x > 0.8$) sections lying in the Si area (note that for the presented instant of time $t = 40$ the coordinates of two convex corners of the boundary are (0.2, 0.5) and (0.8, 0.5), respectively). Naturally, the curve is symmetric about the point $x = 0.5$. Here a maximum with a value of about $20 \cdot 10^{-4}$ is attained. The curve has a linear-parabolic shape and rests on the "shelves" of the background values of concentrations of 10^{-4} in the [0, 0.2] and [0.8, 1] ranges. Curve 2 in Fig. 3c presents the $C(x, y_2)$ distribution on the ray $y_2 = 0.75$ that passes through the Si area ($x < 0.2$ and $x > 0.8$), crosses the segregation fronts at points $x = 0.2$ and $x = 0.8$, and passes through the oxide SiO_2 area ($0.2 < x < 0.8$). Curve 2 is also symmetric about the point $x = 0.5$: in the sections of Si the concentrations have background values of 10^{-4}, at the fronts bursts (peaks) of concentrations up to values of $20 \cdot 10^{-4}$ are observed, and in the SiO_2 area the concentration decreases down to values of 10^{-5} (the segregation law of $m = 20 \cdot 10^{-4}/10^{-5} = 200$ is fulfilled with machine accuracy). In this case, in the SiO subarea there is a section

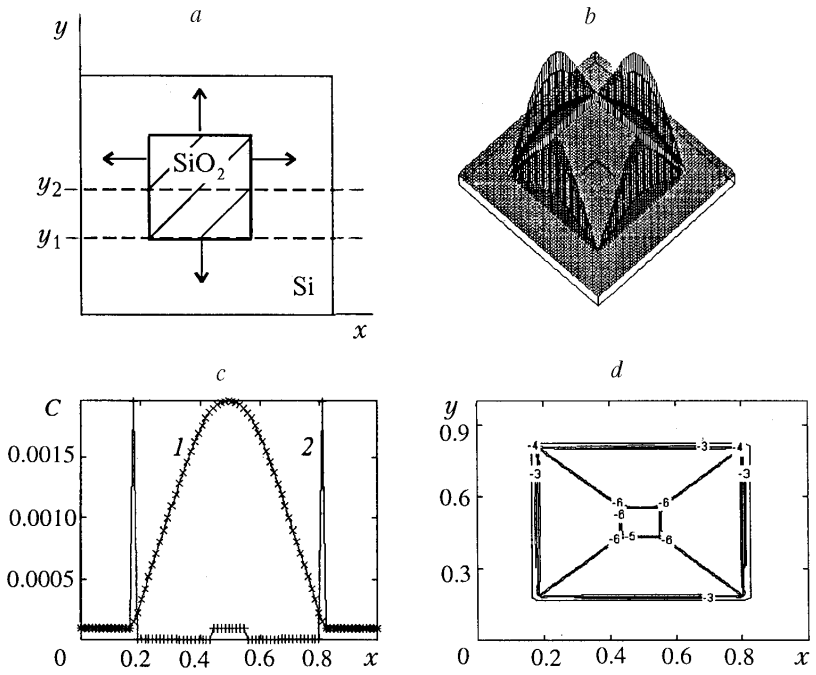

Fig. 4. Segregation on the "square"-type cavity: a) general topology of the problem; b) isometry of $C(x, y)$ concentrations in the calculated area; c) $C(x, y_i)$ distributions (1 and 2 correspond to $y_1 = 0.2$ and $y_2 = 0.5$); d) $C(x, y)$ isolines.

$(0.45 < x < 0.55)$ with background value of concentrations of 10^{-4}, which represents the oxide area at the initial instant of time $t = 0$ (unshaded rectangle in the upper part of Fig. 3a).

The pictures of the $C(x, y)$ distributions on the rays x = const, i.e., in the other coordinate direction, are shown in Fig. 3d. Curve 2 corresponds to the $C(x_2, y)$ values on the symmetry line of the problem $x_2 = 0.5$. This ray (see Fig. 3a) passes through the area of the Si material ($y < 0.5$), crosses the SiO_2/Si front at the point $y = 0.5$, and then passes through the area of the SiO_2 oxide ($y > 0.5$). It should be noted that this occurs in its two subareas — in the subarea in which during the solution of the problem oxidation has occurred ($0.5 < y < 0.75$) and in the oxide subarea ($y > 0.75$). To these areas there correspond variations in the concentration values: in the area of Si, $C(x_2, y)$ has background values of 10^{-4}, at the front there is a burst, and the peak value of $C(x_2, y)$ reaches $20 \cdot 10^{-4}$, in the first subarea of SiO_2 $C(x_2, y)$ decreases to 10^{-5} and in the subarea of the initial oxide $C(x_2, y)$ has a background value of 10^{-4} again.

Curve 1 in Fig. 3d presents the $C(x_1, y)$ values on the ray $x_1 = 0.2$. The latter passes (see Fig. 3a) through the area of the Si material ($y < 0.5$), then goes along the SiO_2/Si wave front ($0,5 < y < 0.8$), and traverses the area of the SiO_2 oxide ($y > 0.8$). Accordingly, in the Si subarea $C(x_1, y)$ has a constant background value of 10^{-4}, and in the second section there is a linear-parabolic increase in the $C(x_1, y)$ values from 10^{-4} to $20 \cdot 10^{-4}$. Note that the curve in this section has a shape analogous to the shape of the central linear-parabolic section of curve 1 in Fig. 3c, and then $C(x_1, y)$ increases up to the maximum value of $26.9 \cdot 10^{-4}$, which is reached in the concave corner of the boundary configuration into which a considerable part of the impurity is ejected similarly to the peak in Fig. 2b. Naturally, in crossing the SiO_2/Si front in the area of the SiO_2 oxide, $C(x_1, y)$ sharply decreases to the background values. It should be recalled that in the SiO_2 subareas, in the sections of its growth in the time interval under consideration, the concentrations that seem to be constant on the given scale with values of $\sim 10^{-5}$, i.e., on curve 2 of Fig. 3c in the ranges of [0.2, 0.45] and [0.55, 0.8] and on curve 2 of Fig. 3d in the [0.5, 0.75] range, vary slightly with a small increase from the initial position of the oxide boundary to the position of the front at the given instant of time, which is only notice-

able with the use of the logarithmic scale (see Figs. 1d and 2c and the comments thereto for the corresponding subareas of concentration distributions).

Segregation on the "Square"-Type Cavity. Unlike the above-discussed configurations, this configuration (see Fig. 4a) represents a closed oxide area surrounded on all sides by the substance area. Note that the geometrical form of the oxidation process of the type of a "square" as well as of the type of a "trench" is often used in the technologies for developing semiconductor materials. In terms of quality, the process of segregation of impurities at the mobile SiO_2/Si boundary is illustrated by the isometry in Fig. 4b. The general picture of the process is characterized by the presence of four fronts that have a linear-parabolic form and move from the center to the periphery.

A quantitave analysis of the distribution of impurity concentrations $C(x, y)$ in the calculated area can be carried out on one-dimensional graphs of $C(x, y_1)$ sections by the rays y = const (Fig. 4c). Curve 1 representing the $C(x, y_1)$ values at time $t = 50$ passes in the areas of the Si material ($x < 0.2$ and $x > 0.8$) and along the SiO_2/Si front ($0.2 < x < 0.8$). As before, the graph of such a dependence is a linear-parabolic function in the second (central) subarea "resting" on the left and on the right on the "shelf" of constant background values of 10^{-4}. The curve is symmetric about the point $x = 0.5$ in which a maximum with a value of $20 \cdot 10^{-4}$ is attained.

Curve 2 (Fig. 4c) shows the $C(x, y_2)$ distribution on one of the symmetry lines of the problem $y_2 = 0.5$. This curve is also symmetric about $x = 0.5$ and has five characteristic sections: a section in Si ($x < 0.2$), intersection of the SiO_2/Si fronts ($x = 0.2$ and $x = 0.8$), and an area in SiO_2 ($0.2 < x < 0.8$) with a subarea of the initial position of the oxide ($0.45 < x < 0.55$). In the Si area and in the subarea of the initial oxide SiO_2, the $C(x, y_2)$ concentrations have background values of 10^{-4}, at the segregation fronts there is a peak with values of $20 \cdot 10^{-4}$, and in the area of SiO_2 after the passage of the oxidation wave the impurity concentration decreases down to 10^{-5} with a slight change in the values, which is only seen on the logarithmic scale (see the last comment on the previous item).

Figure 4d shows the picture of the 2*D*-isolines of $C(x, y)$ at a given instant of time, which complements the 3*D*-isometry of Fig. 4b and the 1*D*-distribution of Fig. 4c. The perfectly smooth sides of the two squares — the internal square presenting the initial position of the SiO_2/Si wave and the external square this wave has reached by $t = 50$ — are well visualized. The diagonal "stripes" represent the trajectory "traces" of motion of the configuration corners as kink points of the impurity concentration function along the parameter of the "square."

Thus, in the present work a numerical simulation of the physicochemical process of segregation of impurities of V(a)-subgroup chemical elements (phosphorous P, arsenic As, and antimony Sb) at the oxidation wave of silicon Si has been performed and complex pictures of the distributions of P, As, and Sb concentrations in the areas of Si and SiO_2 and at the SiO_2/Si front have been obtained and analyzed.

NOTATION

$m = C_+/C_-$, segregation coefficient; C, impurity concentration; C_+, impurity concentration at the material/oxide boundary on the side of the material; C_-, same on the side of the oxide; x, y, Cartesian coordinates of the problem; t, time. Subscripts: 1, 2, 3 correspond to the curve numbers in the figures.

REFERENCES

1. A. G. Tarnavskii, S. I. Shpak, and M. S. Obrekht, *Vych. Met. Program.*, **2**, No. 1, 12–26 (2001). http://www.srcc.msu.su/num- meth.
2. C. P. Ho and J. D. Plumber, *J. Electrochem. Soc*., **126**, No. 9, 1516–1522 (1979).

3. C. P. Ho and J. D. Plumber, *J. Electrochem. Soc*., **126**, No. 9, 1523–1530 (1979).
4. C. P. Ho, J. D. Plumber, and J. D. Meindl, *J. Electrochem. Soc*., **125**, No. 4, 665–671 (1978).
5. D. Chin, S. Y. Oh, S. M. Hu, R. W. Dutton, and J. L. Moll, *IEEE Trans., Elec. Dev*., **ED-30**, No. 7, 744–749 (1983).
6. C. S. Rafferty, *Stress Effects in Silicon Oxidation. Simulation and Experiments*, Doctoral Dissertation, Stanford Univ., Stanford, CA (1989).
7. V. I. Kol'dyaev, V. A. Moroz, and S. A. Nazarov, *Avtometriya*, No. 3, 46–54 (1988).
8. V. N. Chebotin, *Physical Chemistry of Solids* [in Russian], Moscow (1982).
9. G. É. Tsyrlin, P. Werner, G. Gosele, B. V. Volovik, V. M. Ustinov, and N. N. Ledentsev, *Pis'ma Zh. Tekh. Fiz*., **27**, Issue 1, 31–38 (2001).
10. E. V. Astrova, V. V. Ratnikov, A. D. Remenyuk, A. G. Tkachenko, and I. L. Shul'pina, *Pis'ma Zh. Tekh. Fiz*., **27**, Issue 2, 1–8 (2001).